

Back reflector influence on the parameters of infrared light-emitting diodes based on AlGaAs/GaAs heterostructure

© A.V. Malevskaya, N.A. Kalyuzhnyy, R.A. Saliy, F.Yu. Soldatenkov, M.V. Nakhimovich, D.A. Malevskii

Ioffe Institute, St. Petersburg, Russia
E-mail: amalevskaya@mail.ioffe.ru

Received April 9, 2024

Revised May 23, 2024

Accepted May 27, 2024

Investigations of back reflectors technology development for IR (850 nm) light-emitting diodes based on AlGaAs/GaAs heterostructures with multiple quantum wells, grown by metalorganic vapor-phase epitaxy, have been carried out. Reflectors constructions based on multi-layer systems included layers of dielectric (SiO_2), adhesive material (NiCr), metal with high reflector properties (Ag) and barrier stop-layers (Ti, Pt) have been developed. Analyzed was the influence of reflector compound on light-emitting diodes parameters. External quantum efficiency $> 45\%$ at current 100–350 mA and optical power > 450 mW at current 800 mA were achieved.

Keywords: IR light-emitting diode, AlGaAs/GaAs heterostructure, multi-layer reflector.

DOI: 10.61011/TPL.2024.09.59159.19946

Infrared (IR) light-emitting diodes (LEDs) are used widely in various fields: optical diagnostics, optical communications, night-vision security systems, and optical sensors of wireless devices [1–4]. The key developments in the field of fabrication of highly efficient high-power IR LEDs are associated with multipass heterostructures with multiple quantum wells (QWs) grown by metalorganic vapor-phase epitaxy (MOVPE). One way to increase the optical power of LEDs is to embed an internal Bragg reflector (BR) or a metal reflector (MR) between the active region and the GaAs substrate absorbing near IR radiation. A BR is embedded monolithically into the epitaxial structure, and the reflection coefficient exceeds 90% under normal radiation incidence at a wavelength of 850 nm. However, a deviation of the incidence angle from 90° reduces the fraction of radiation reflected from the BR (reflection proceeds in a solid angle with an opening of $\pm 20^\circ$) [5,6]. The technology of embedding metal reflectors into the LED structure involves the transfer of a heterostructure with a deposited reflector onto a carrier substrate [7,8]. Various reflector systems based on layers of Ag, ITO/Ag (ITO is indium tin oxide), Ti/ITO/Ag, Ti/Au, Al/Au, Cu/Au, and Ni/Au, which reflect ~ 92 – 97% of incident radiation, are known [9–11]. A large number of process operations performed in the technological cycle of MR embedding may exert a negative influence on the optical characteristics of reflectors. For example, the formation of ohmic contacts of LEDs includes a stage of thermal annealing at temperatures up to 400°C , which may lead to fusion of the reflector material into the semiconductor structure and, consequently, to a reduction in the coefficient of reflection of incident radiation. The technology of transfer of a heterostructure onto a carrier substrate involves fusing a binder compound based on Au and In layers. A monolithic intermetallic compound forms in this case, binding the carrier substrate

to the heterostructure. However, owing to a high diffusion coefficient, In may penetrate into the reflector layers and affect its optical properties negatively, and the emergence of microdefects in the Au–In alloy [12] may raise the level of resistive losses in the device.

The aim of the present study is to (1) design a built-in LED reflector that reflects more than 96–98% of incident radiation; (2) analyze the technological stages of LED fabrication that exert a negative influence on the optical properties of reflectors; and (3) examine the influence of technological parameters on the optical power of finished devices.

Test LEDs were manufactured on the basis of AlGaAs/GaAs heterostructures with multiple QWs grown by metalorganic vapor-phase epitaxy on *n*-type GaAs substrates. The heterostructure includes an active region with six InGaAs QWs positioned at the center of an $\text{Al}_{0.2}\text{Ga}_{0.8}\text{As}$ wide-band layer with a thickness greater than $1\ \mu\text{m}$; barrier *n*- and *p*-type $\text{Al}_{0.4}\text{Ga}_{0.6}\text{As}$ layers; an additional back wide-band *n*- $\text{Al}_{0.9}\text{Ga}_{0.1}\text{As}$ layer 300 nm in thickness (with a refraction index lower than the one in narrow-band $\text{Al}_{0.2-0.4}\text{Ga}_{0.6-0.8}\text{As}$ layers) that reflects rays with such angles of incidence under which total internal reflection is observed; *n*- $\text{Al}_{0.2}\text{Ga}_{0.8}\text{As}$ and *p*- $\text{Al}_{0.2}\text{Ga}_{0.8}\text{As}$ layers that ensure current spreading; and heavily doped contact *n*⁺-GaAs and *p*⁺-GaAs layers with front and back ohmic contacts to them. A sacrificial $\text{Al}_{0.9}\text{Ga}_{0.1}\text{As}$ layer was grown in order to transfer the heterostructure onto the carrier substrate and remove the growth substrate. Wet chemical etching of this layer is highly selective with respect to etching of the GaAs growth substrate.

The reflector embedding technology includes the following stages: formation of point contacts $10\ \mu\text{m}$ in diameter with a pitch of $75\ \mu\text{m}$; etching of the *p*⁺-GaAs contact layer in regions free from point contacts; deposition of

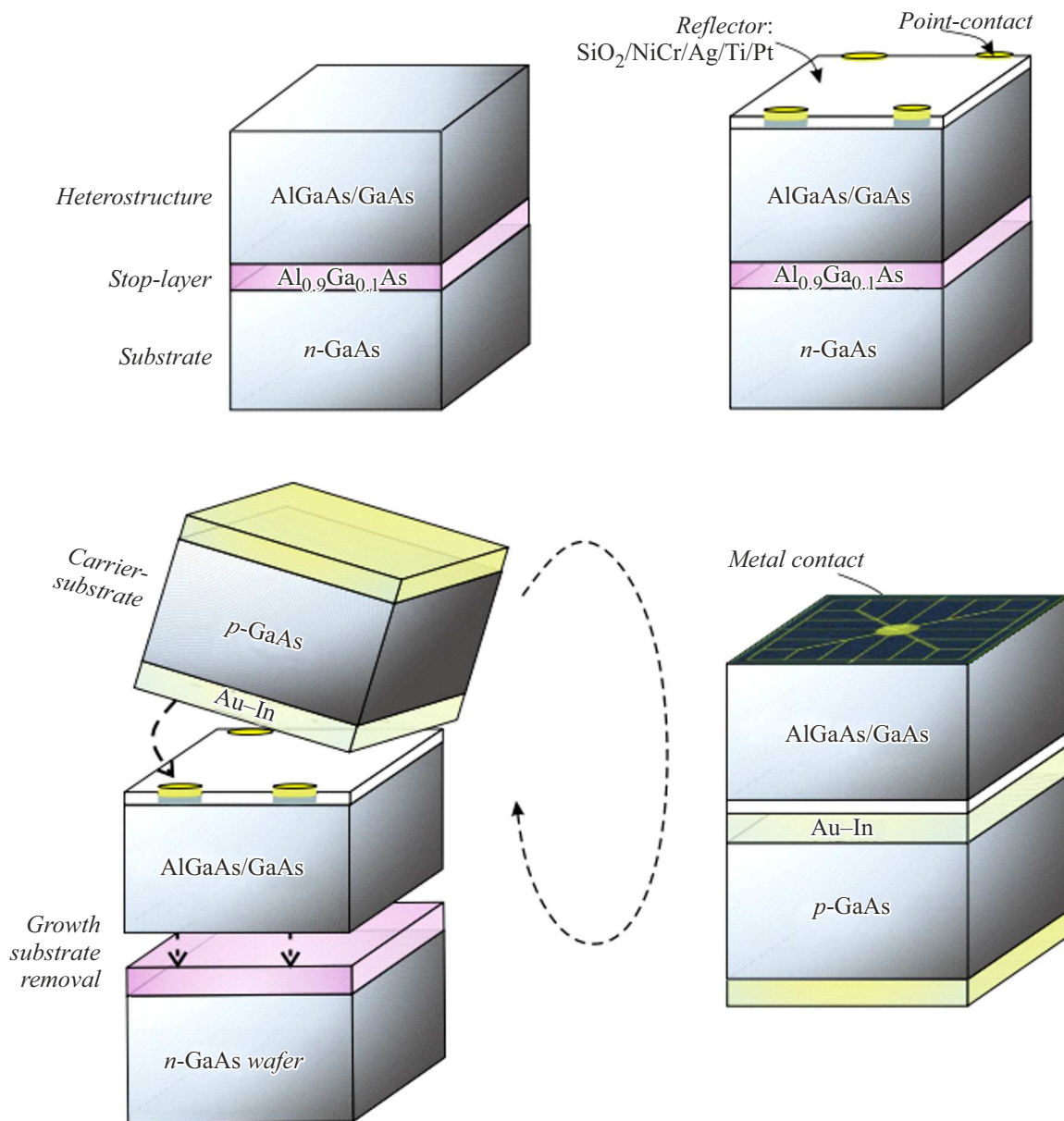


Figure 1. Schematic diagram of different stages of embedding a metal reflector by transferring a heterostructure onto a carrier substrate.

MR layers; transfer of the heterostructure onto the *p*-GaAs carrier substrate with the use of the Au–In compound; removal of the growth substrate; texturing of the front light-emitting surface; formation of the front ohmic contact; and etching of the LED separation mesa (Fig. 1).

The technology of embedding of the MR exerts a profound influence on its optical properties and, consequently, on the LED optical power. A study of the formation of reflectors based on Ag and Au with and without various types of adhesion layers was conducted. Experiments were carried out by depositing MR layers onto a cover glass 140 μm in thickness with subsequent measurement of the reflection coefficient both from the glass side and from the side of reflector layers. Earlier studies [6] have revealed that the deposition of Ag or Au layers without adhesive layers

results in the formation of a non-monolithic LED structure due to detachment of the reflector layers. However, the deposition of a NiCr alloy layer 0.5–1 nm in thickness has no negative effect on the reflector optical properties and allows one to form a reflector with high adhesion to the semiconductor structure. The reflection coefficient measured under normal incidence of radiation onto glass decreased significantly (by 7%) due to losses in Fresnel reflection and absorption of a fraction of radiation in the glass. The reflection coefficient from the glass and Ag sides was 90–91% (curve 1 in Fig. 2, *a*) and 97–98% (curve 2 in Fig. 2, *a*), respectively, at radiation wavelengths of 700–1000 nm.

The transfer of the heterostructure onto the GaAs carrier substrate involves fusing the In layer deposited onto the

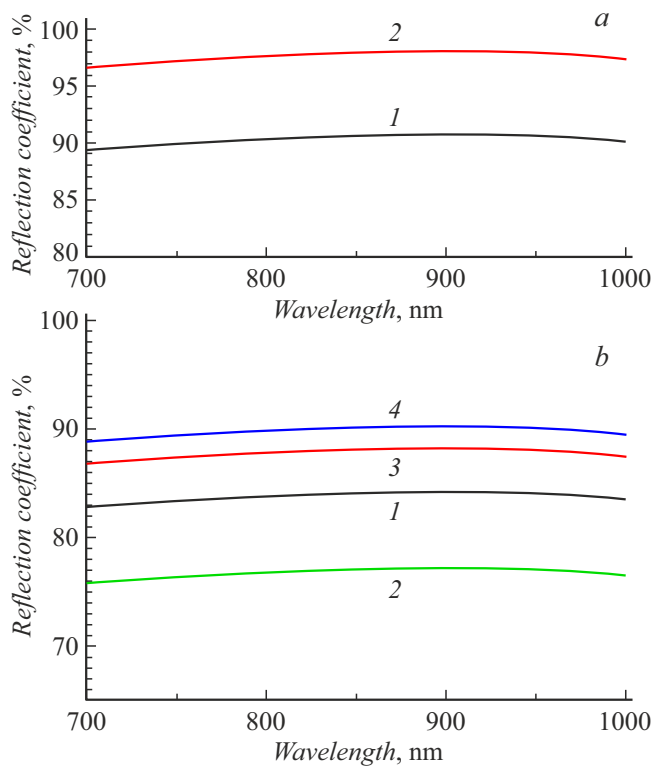


Figure 2. Spectral dependence of the coefficient of radiation reflection from the MR based on NiCr–Ag (*a*) measured through glass (*1*) and from the Ag reflector side (*2*) and the same dependence after indium diffusion (*b*) measured through glass without a barrier layer (*1*) and with barrier layers of NiCr (20 nm) (*2*), Ti (50 nm) (*3*), Ti (50 nm)+Pt (50 nm) (*4*).

carrier substrate with the Au layer deposited onto the reflector surface. The optical properties of a reflector based on NiCr (0.5–1 nm)–Ag layers were determined in order to study the diffusion of indium. The following experiment was performed: reflector, gold, and indium layers with a thickness of $2\ \mu\text{m}$ were deposited onto glass, and the structure was annealed at a temperature of 200°C for 30 min. The spectral dependence of the reflection coefficient under normal incidence of radiation onto the sample was measured before and after thermal annealing. The reflection coefficient measured through glass (curve *1* in Fig. 2, *b*) was 90–91% before annealing and 83–84% after annealing within the 700–1000 nm wavelength range. A 7% reflection coefficient reduction is indicative of partial diffusion of indium into the reflector layers during thermal annealing.

Various types of barrier layers were introduced between the silver reflector and indium to protect the former from indium diffusion: NiCr (20 nm), Ti (50 nm), and Ti (50 nm) + Pt (50 nm). Experimental samples were manufactured as above, but with the addition of barrier layer deposition.

The use of NiCr as a barrier layer (curve *2* in Fig. 2, *b*) resulted in a significant reduction of the reflection coefficient

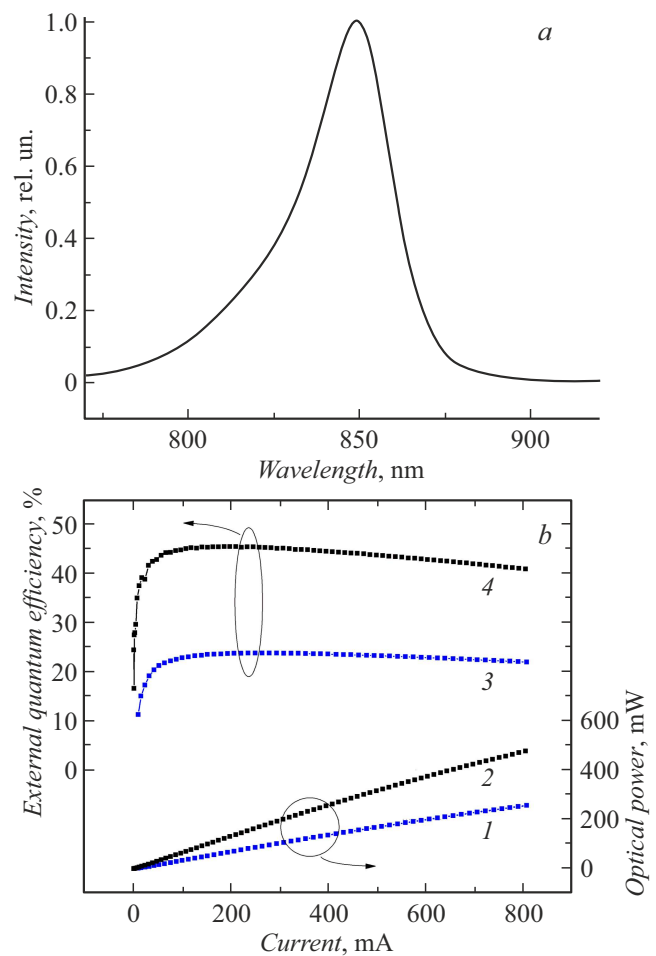


Figure 3. Spectral characteristic (*a*) and dependence of EQE and optical power (*b*) of IR LEDs with a back reflector without barrier layers (*1*, *3*) and with Ti + Pt barrier layers (*2*, *4*).

(compared even to an MR without a barrier layer), which may be attributed to the additional diffusion of chromium into the reflector layers. The highest reflection coefficient (89–90%), which was virtually the same as the one measured prior to indium diffusion (curve *1* in Fig. 2, *a*) was obtained with the use of barrier layers based on Ti (50 nm) + Pt (50 nm) (curve *4* in Fig. 2, *b*). The use of a Ti layer (50 nm) only resulted in a slight (2%) reduction of the coefficient of reflection of incident radiation (curve *3* in Fig. 2, *b*). Thus, the formation of Ti + Pt barrier layers between the MR and indium prevents the diffusion of indium into the reflector layers and ensures preservation of its initial optical properties, providing an opportunity to maximize the optical power of IR LEDs.

A technique for preventing the degradation of optical properties of the MR in the course of fusing of its layers into a semiconductor structure in high-temperature processes was developed. Thermal annealing is performed in LED manufacture both in the process of Au and In fusing and during the formation of a front ohmic contact to *n*-type layers. The deposition of an additional dielectric

layer between the MR layers and the heterostructure was proposed. The dielectric coating material was selected based on its refraction index: when a dielectric layer with a minimum refraction index is deposited, the angle of total internal reflection decreases, which leads to an increase in the fraction of radiation incident at angles greater than the angle of total internal reflection. The deposition of an additional SiO₂ ($n \approx 1.4$) dielectric layer both improves the optical properties of a reflector and prevents the fusion of metallic reflector materials into the semiconductor.

IR LED crystals with a radiation wavelength of 850 nm (Fig. 3, *a*) with a built-in metal reflector with different layer compositions were manufactured. The first reflector design included a SiO₂ (400 nm) dielectric layer, a NiCr (0.5–1 nm) adhesion layer, and an Ag (200 nm) reflective layer. The second design featured additional Ti (50 nm) + Pt (50 nm) barrier layers formed on the Ag surface. In preparation for measurements, LED crystals were mounted on ceramic heat-dissipating bases and packaged into an optical element in the form of a silicone hemisphere.

The IR LED parameters were measured in the pulsed current mode ($\tau_{imp} = 5\text{--}300\ \mu\text{s}$): the voltage across the crystal and the luminous flux from LEDs (determined from the photocurrent of the reference photodetector with a known spectral photosensitivity) were recorded. The obtained values were used to calculate the external quantum efficiency and optical power of LEDs as functions of the applied current.

Optical power levels $> 250\ \text{mW}$ at a current of 800 mA (curve 1 in Fig. 3, *b*) were observed for LED samples fabricated without barrier layers; the maximum external quantum efficiency (EQE) was 23% at a current of 100–500 mA (curve 3 in Fig. 3, *b*). The technology of fabrication of LED reflectors with Ti + Pt barrier layers provided an almost two-fold enhancement of EQE (to levels in excess of 45%) at a current of 100–350 mA (curve 4 in Fig. 3, *b*), while the output optical LED power was raised to 450 mW at a current of 800 mA (curve 2 in Fig. 3, *b*).

The technology of formation of built-in multilayer MRs based on NiCr–Ag layers for IR LEDs manufactured by transferring the heterostructure onto a GaAs carrier substrate with the use of the Au–In In compound was studied. It was demonstrated that the diffusion of indium from the Au–In alloy during post-growth LED heating has a significant impact on the optical properties of the embedded MR, reducing its reflection coefficient by 7%. The use of Ti (50 nm) + Pt (50 nm) barrier layers, which prevent diffusion processes during heating of the LED structure, allowed us to achieve an MR reflection coefficient of 97–98% within the 700–1000 nm wavelength range. IR LEDs manufactured with barrier layers demonstrated a two-fold increase in external quantum efficiency ($> 45\%$) and an optical power $> 450\ \text{mW}$ at a current of 800 mA.

Conflict of interest

The authors declare that they have no conflict of interest.

References

- [1] A.G. Entrop, A. Vasenev, *Energy Proc.*, **132**, 63 (2017). DOI: 10.1016/j.egypro.2017.09.636
- [2] M. Kitamura, T. Imada, S. Kako, Y. Arakawa, *Jpn. J. Appl. Phys.*, **43**, 2326 (2004). DOI: 10.1143/JJAP.43.2326
- [3] W. Wild, *Proc. Est. Acad. Sci. Eng.*, **13**, 436 (2007). DOI: 10.3176/eng.2007.4.15
- [4] A.C. Watts, V.G. Ambrosia, E.A. Hinkley, *Remote Sens.*, **4**, 1671 (2012). DOI: 10.3390/rs4061671
- [5] S.-C. Ahn, B.-T. Lee, W.-C. An, D.-K. Kim, I.-K. Jang, J.-S. So, H.-J. Lee, *J. Korean Phys. Soc.*, **69**, 91 (2016). DOI: 10.3938/jkps.69.91
- [6] A.V. Malevskaya, N.A. Kalyuzhnyy, D.A. Malevskii, S.A. Mintairov, R.A. Saliy, A.N. Pan'chak, P.V. Pokrovskii, N.S. Potapovich, V.M. Andreev, *Fiz. Tekh. Poluprovodn.*, **55** (7), 614 (2021) (in Russian). DOI: 10.21883/FTP.2021.07.51028.9646
- [7] A.V. Malevskaya, N.A. Kalyuzhnyy, D.A. Malevskii, S.A. Mintairov, A.M. Nadtochiy, M.V. Nakhimovich, F.Y. Soldatenkov, M.Z. Shvarts, V.M. Andreev, *Semiconductors*, **55** (8), 686 (2021). DOI: 10.1134/S1063782621080121.
- [8] A.V. Malevskaya, N.A. Kalyuzhnyy, F.Y. Soldatenkov, R.V. Levin, R.A. Saliy, D.A. Malevskii, P.V. Pokrovskii, V.R. Larionov, V.M. Andreev, *Tech. Phys.*, **68** (1), 161 (2023). DOI: 10.21883/TP.2023.01.55451.166-22.
- [9] H.-J. Lee, G.-H. Park, J.-S. So, C.-H. Lee, J.-H. Kim, L.-K. Kwac, *Infrared Phys. Technol.*, **118**, 103879 (2021). DOI: 10.1016/j.infrared.2021.103879
- [10] H.-J. Lee, I.-K. Jang, D.-K. Kim, Y.-J. Cha, S.W. Cho, *Micromachines*, **13**, 695 (2022). DOI: 10.3390/mi13050695
- [11] H.-J. Lee, G.-H. Park, J.-S. So, J.-H. Kim, H.-G. Kim, L.-K. Kwac, *Current Appl. Phys.*, **22**, 36 (2021). DOI: 10.1016/j.cap.2020.12.002
- [12] N.A. Kalyuzhnyy, A.V. Malevskaya, S.A. Mintairov, M.A. Mintairov, M.V. Nakhimovich, R.A. Saliy, M.Z. Shvarts, V.M. Andreev, *Solar Energy Mater. Solar Cells*, **262**, 112551 (2023). DOI: 10.1016/j.solmat.2023.112551

Translated by D.Safin